Choi, H. K., "Energy Distribution and Heat Transfer in an Argon Transferred-Arc Reactor," Ph.D. Thesis, McGill University (1981).
Devoto, R. S., "Transport Coefficients of Partially Ionized Argon," *The Physics of Fluids*, **10**, (2), 354 (1967).
Eddy, T. L., E. Pfender, and E. R. G. Eckert, "Spectroscopic Mapping of the Nonequilibrium Between Electron and Excitation Temperatures in a 1 Atm Helium Arc," *IEEE Trans. on Plasma Science*, **PS-1**, (4), 31 (1973).
Fauchais, P., "Utilisation Industrielle Actuelle et Potentielle des Plasmas," *Revue Phys. App.*, **15**, 1281 (1980).
Fink, J. E., "Theory and Computation of the Characteristics of the Thermal Electrical Plasma Arc for Chemical Engineering Applications," *Chem. Eng. Commun.*, **5**, 37 (1980).
Gauvin, W. H., G. R. Kubanek, and G. Irons, "The Plasma Production of Ferromolybdenum—Process Development and Economics," *J. of Metals*, 42 (Jan., 1981).
Grey, J., P. F. Jacobs, and M. P. Sherman, "Calorimetric Probe for the Measurement of Extremely High Temperatures," *Rev. Sci. Instrum.*, **33**, (7), 738 (1962).
Grey, J., "Thermodynamic Methods of High-Temperature Measurement," *ISA Trans.*, **4**, 102 (1965).
Grey, J., "Proposed Method for Measuring Gas Enthalpy using Calorimetric Probes," ASTM, Committee E-21 on Space Simulation (1968).
Guile, A. E., "Arc-Electrode Phenomena," *IEEE Reviews*, **118**, 1131 (1971).
Hamblyn, S. M. L., "A Review of Applications of Plasma Technology with Particular Reference to Ferro-Alloy Production," National Inst. for Metallurgy, Report No. 1895 (1977).
Johnson, D. C., and E. Pfender, "Modelling and Measurement of the Initial Anode Heat Fluxes in Pulsed High Current Arcs," *IEEE Trans. on Plasma Sci.*, **PS-7**, (1), 44 (1979).
Liu, C. H., and E. Pfender, "Heat Transfer in the Anode Region of High Intensity Arcs," *Studies in Heat Transfer*, A Festschrift for E. R. G. Eckert, Hemisphere Publ. Corp., Washington (1979).
Lochte-Holtgreven, W., *Plasma Diagnostics*, North-Holland Publ. Co., Amsterdam (1968).
Mehmetoğlu, M. T., F. Kitzinger, and W. H. Gauvin, "A Novel Technique of Plasma Temperature Measurement," *Rev. Scient. Instrum.*, **53**, No. 3, 285–293 (1982).
Olsen, H. N., "Determination of Properties of an Optically Thin Ar Plasma," *Temperature: Its Measurement and Control in Science*, **3**, 593 (1962).
Rykalin, N. N., "Plasma Engineering in Metallurgy and Inorganic Materials Technology," *Pure and Appl. Chem.*, **48**, 179 (1976).
Sayce, I. G., and B. Selton, "Special Ceramics," ed., P. Popper, British Ceramic Research Assoc., Stoke-on-Trent, 157 (1972).
Sayce, I. G., "Some Applications of Thermal Plasmas to Material Processing," paper 107, Section 4A, World Electrotechnical Congress, Moscow (July, 1977).
Sheer, C., S. Korman, C. G. Stojanoff, and P. S. Tschang, "Diagnostic Study of the Fluid Transpiration Arc," Mechanical Div., Air Force Office of Sci. Res., AFOSR 70-0195 TR (1969).
Sheer, C., S. Korman, and S. F. Kang, "Investigation of Convective Arcs for the Simulation of Re-entry Aerodynamic Heating," Aeromechanics Div., Air Force Office of Sci. Res. (1973).
Smith, J. L., and E. Pfender, "Determination of Local Anode Heat Fluxes in High Intensity Thermal Arcs," *IEEE Trans. on PAS*, **PAS-95**, (2), 704 (1976).
Stojanoff, C. G., "A Transient Fiber Optics Probe for Space Resolved Diagnostics of Dense Plasmas," *AIAAJ*, **4**, (10), 1766 (1966).
Stojanoff, C. G., "Characteristics of an Axially Flow Stabilized Arc and Its Application to the Determination of Transport Properties," Ph.D. Thesis, Stuttgart University, (in German) (1968).
Wilkinson, J. B., and D. R. Milner, "Heat Transfer from Arcs," *Brit. Welding*, 115 (1960).

Manuscript received May 13, 1981; revision received March 9, and accepted March 23, 1982.

Turbulent Velocity Fluctuations That Control Mass Transfer to a Solid Boundary

J. A. CAMPBELL and T. J. HANRATTY

University of Illinois Urbana, IL 61801

The relation between the velocity and concentration fields for a fully developed turbulent flow which transfers mass to a pipe wall at large Schmidt numbers has been studied. Measurements of the fluctuations of the concentration gradient and the velocity gradient were obtained simultaneously at multiple locations on the wall. Spatial scales were calculated for the low frequency velocity fluctuations by passing the measured signals through low-pass filters. These scales are the same size as the scales of the concentration fluctuations. This result provides additional support for the notion that mass transfer to a boundary at high Schmidt numbers is controlled by low frequency velocity fluctuations which contain only a small fraction of the total turbulent energy.

SCOPE

A recent analysis by Campbell and Hanratty (1981a) using the linearized form of the mass balance equation for a turbulent flow shows that the magnitude of the Reynolds transport term is controlled by low frequency velocity fluctuations containing a small fraction of the total turbulent energy. The work described in this paper was carried out to see whether this interpretation is consistent with measurements of the scale of the turbulence and whether such low frequency velocity fluctuations are universal properties of the turbulence.

The structure of the velocity field close to a wall was studied by measuring the transverse component of the fluctuating velocity gradient simultaneously at multiple locations on the wall. By low-pass filtering the signals from these probes it is possible to compare the spatial scale of the low frequency velocity gradient fluctuations with the spatial scale of the full signal and with the spatial scale of the concentration fluctuations. By examining the measurements of the mass transfer fluctuations in different systems, it is possible to determine whether these fluctuations are strongly dependent on the design of the flow system.

CONCLUSIONS AND SIGNIFICANCE

The transverse scale of the low frequency velocity fluctuations is found to be approximately equal to the transverse scale of the concentration fluctuations at the wall. Furthermore, velocity fluctuations of all frequencies appear to have the same transverse scale. We therefore conclude that there is no contradiction between measurements of the spatial scale of the mass transfer fluctuations and the notion that turbulent mass transfer to a solid boundary at large Schmidt numbers is controlled by velocity fluctuations of much lower frequency than those containing most of the energy.

The good agreement between the measurements (frequency spectra and intensities) of mass transfer fluctuations in a 20-cm pipe described in this paper and previous measurements in a 2.54-cm pipe indicates they are universal properties and turbulence and not strongly affected by the particular design of the experimental flow system.

Further support for the notion that low frequency velocity fluctuations are controlling mass transfer rates has been obtained from numerical solutions of the nonlinear mass balance equation using a randomly varying velocity input (Campbell and Hanratty, 1981b). The results presented in this paper have been of particular use in this nonlinear analysis by defining a scale to characterize the transverse convection term.

INTRODUCTION

Turbulent mass transfer between a flowing fluid and a solid boundary at high Schmidt numbers is characterized by a concentration boundary layer which is so thin that it lies entirely within the viscous sublater ($\delta_c^+ < y \rightarrow u = \alpha(x,z,t)y$ 5), where the components of the velocity are given as $u = \alpha(x,z,t)$, $v = \beta(x,z,t)y^2$ and $w = \gamma(x,z,t)y$. The variation of the velocity field within the concentration boundary layer is described totally by the velocity gradients α and γ, since β is related to α and γ through the equation of conservation of mass.

The development of techniques to measure both components of the fluctuating velocity gradient at the wall (Reiss and Hanratty, 1962, 1963; Mitchell and Hanratty, 1966; Sirkar and Hanratty, 1970) and fluctuations in the local rate of mass transfer (Van Shaw and Hanratty, 1964) have provided an opportunity to relate turbulent mass transfer to the properties of the fluctuating flow in the immediate vicinity of a solid boundary. However, these studies as well as more recent researches (Shaw and Hanratty, 1977a,b; Lee, Eckelman and Hanratty, 1974) have yielded results which appear contradictory.

Measurements of the fluctuating flow close to a boundary reveal flow structures, approximately homogeneous in the flow direction, which are characterized by a transverse length of $\lambda^+ \cong 100$ and by a period of $T^+ \cong 100$. Measurements of fluctuations in the mass transfer rate to the wall at large Schmidt numbers reveal structures with dimensions similar to those observed for the velocity field (Shaw and Hanratty, 1977a) but with a characteristic frequency, at least an order of magnitude smaller, which decreases with increasing Schmidt number.

One possible interpretation of the above results is that the mass transfer is being controlled by the most energetic velocity fluctuations; i.e., the flow oriented wall eddies identified in a number of laboratories. Concentration fluctuations associated with these velocity fluctuations are highly damped near the wall so this interpretation also suggests that the measured mass transfer fluctuations at the wall are only weakly connected with the net turbulent transport of mass. This viewpoint receives support from the observation by Shaw and Hanratty (1977a) that the spatial scale of the mass transfer fluctuations in the transverse direction is not sensitive to changes in Schmidt number.

To the contrary, a recent analysis by Campbell (1981) using the linearized form of the mass balance equation shows that the frequency spectrum of the Reynolds transport term is characterized by much lower frequencies than the most energetic velocity fluctuations. This suggests that the mass transfer boundary layer acts as a filter so that as the Schmidt number increases, smaller and smaller fractions of the energy of the velocity field are effective in turbulent transport. Thus, at a $S = 1000$ only ~15% of the energy associated with the velocity fluctuations normal to the wall and 3% at $S = 50{,}000$ are effective in transporting mass. This interpretation raises interesting questions regarding the low frequency velocity fluctuations. Do they have a transverse scale of $\lambda^+ = 100$ as suggested by the correlation measurements of Shaw and Hanratty (1977a)? Are these low frequency velocity fluctuations universal properties of the turbulence or are they associated with the particular design of the system in which the measurements are obtained?

This paper presents the results of experiments carried out to answer the above questions.

EXPERIMENTS

The experiments were conducted in a vertical flow system which provides a straight entrance length of 15 m for a circular test section 20 cm in diameter (Sirkar, 1969). The test fluid was an aqueous solution of iodine, potassium iodide, and sodium sulfate.

The transverse component of the velocity gradient at the wall, $\gamma(x,z,t)$ was measured in a Plexiglas test section at different transverse locations with electrochemical techniques developed in this laboratory (Reiss, 1962; Sirkar, 1969). As shown in the paper cited above, the simultaneous measurements of $\gamma(x,z,t)$ at multiple locations allows for the identification of a "wavelike" pattern with a distance between zero crossings of positive (or of negative) slope of $\lambda^+ = 100$. These can be interpreted as being associated with a secondary flow superimposed on the main flow of the type depicted in the idealized eddy pattern shown in Figure 1. By using low pass filters on the signals coming from the multiple probes, it was possible to study the spatial variation of the low frequency portion of the velocity signals which seem to be controlling turbulent mass transfer at high Schmidt numbers.

As described in previous articles (Sirkar and Hanratty, 1970; Lee, Eckelman and Hanratty, 1974; Fortuna and Hanratty, 1972) the velocity gradient at the wall was measured using a pair of rectangular electrodes mounted flush with the wall in a chevron arrangement. The dimensions of the electrode pairs used in this work are given in Figure 2. They consisted of platinum sheets epoxied into slits milled in the wall of the pipe. Details of the construction are given by Hogenes (1979). These electrodes were cathodes of an electrolysis cell at which the following reaction occurred:

$$I_3^- + 2e^- \rightarrow 3I^-.$$

At large enough cathode voltages the measured current can be related to the velocity gradient at the wall. The sum of the signals from the two electrodes gives the component of the velocity gradient in the direction of mean flow and the difference, the component in the transverse direction. Forty pairs of these electrodes were spaced around the pipe circumference but only nine of these were used in this experiment. The signals were sampled at a frequency of 40 Hz or $n_s^+ = 1.4$ for 8,000 samples. The results are digitized and stored in a computer. Discussion of the frequency response and spatial resolution of the velocity gradient probes are to be found in the references cited above.

In the mass transfer experiments the test section, which was the cathode of an electrolysis cell, consisted of a section of nickel pipe 20 cm in diameter that was plated with platinum. Anodes were located in the flow system as shown in Figure 3. The downstream anode consisted of 25 stainless steel sheets with 15 m^2 of surface area. The other anode, located 102 cm upstream of the test section, was a 28 cm section of brass pipe plated with nickel. At high enough voltages the current flowing through the cell, I, is

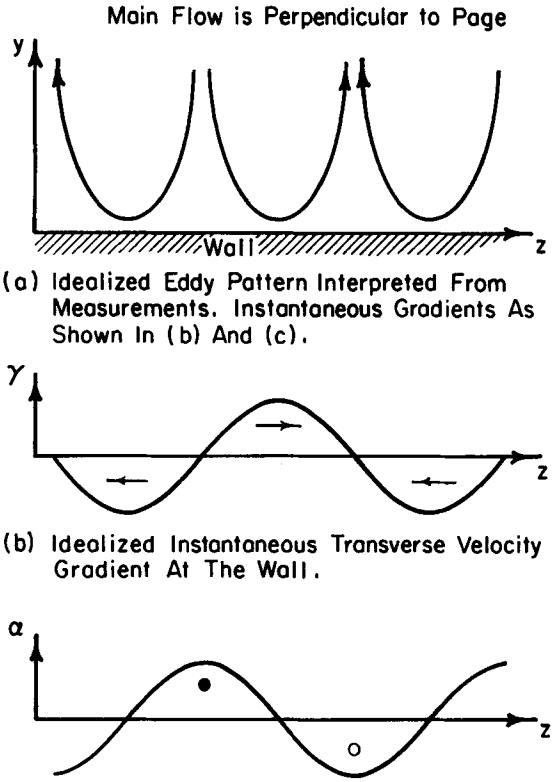

Figure 1. Representation of the near-wall velocity field as pairs of regular streamwise eddies.

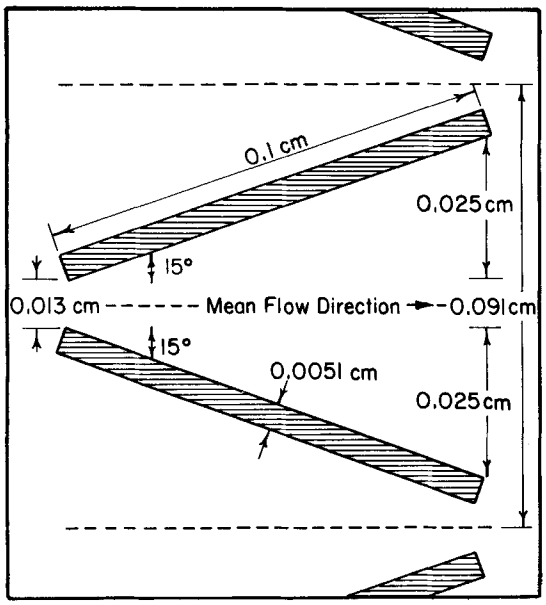

Figure 2. Design of chevron probe for measurement of streamwise and transverse velocity gradients at the wall.

controlled by the rate of mass transfer to the test section. The mass transfer coefficient is therefore calculated as

$$K = \frac{I}{n_e F C_B A} \tag{1}$$

where n_e is the number of electrons involved in the reaction, F, Faraday's constant, C_B, the bulk concentration of iodine, and A, the cathode area.

Local mass transfer rates to the surface of the test section were measured from gold wires mounted flush with it's surface, and electrically insulated from the surface by a thin layer of epoxy. These probes were located 33 cm from the upstream edge of the test section in the arrangement shown in

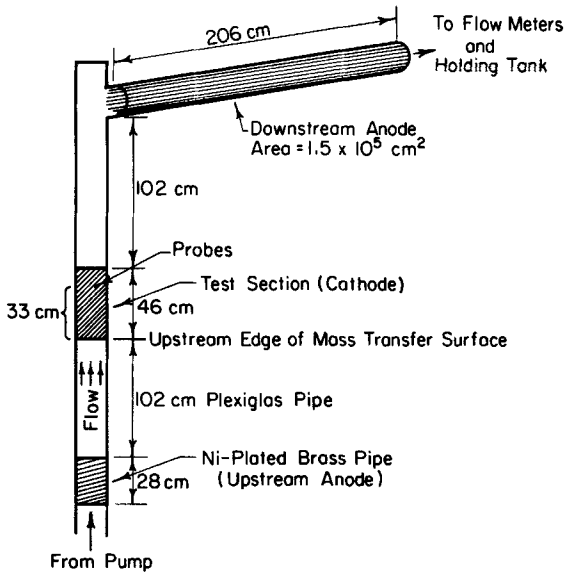

Figure 3. Placement of cathode and anode for measurement of the mass transfer coefficient.

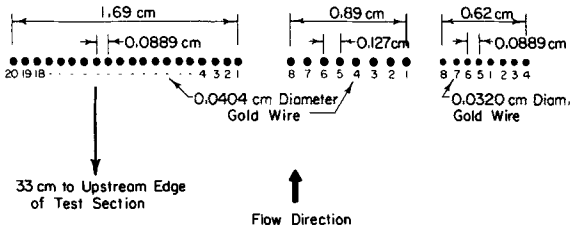

Figure 4. Placement of isolated probes for measurement of local mass transfer coefficient.

TABLE 1. PHYSICAL AND SOLUTION PROPERTIES FOR EXPERIMENTAL RUNS

Property	γ	$\overline{K}$
C_{KI} (mol/L)	0.1	0.25
C_{I_2} (mol/cm^3) $\times 10^7$	18.6–60.0	2.025
$C_{Na_2SO_4}$ (mol/L)	0	0.07
Re	12,500–18,200	20,200–39,700
S	744	792
D (cm^2/s) $\times 10^5$	1.138	1.102
u^* (cm/s)	0.464	0.527–0.951
ν (cm^2/s)	0.00847	0.00873

Figure 4. These probes were sampled at 3 to 10 Hz($n_s^+ \cong 0.1$) to obtain 10,000 data points. Before digitization the mean was removed from the signal, the fluctuations amplified, and very high frequency noise removed. The results were stored in a computer for future use. Details regarding the measuring techniques including discussions of the frequency response and spatial resolution, are contained in previous papers (Shaw and Hanratty, 1977a,b) from this laboratory and in a thesis by one of the authors (Campbell, 1981).

The physical properties of the electrolyte used in these studies are listed in Table 1. The mass transfer experiments were conducted at a Schmidt number, S, of 792. Sodium sulfate was added to the electrolyte in these runs to increase its electrical conductivity. When the voltage drop through the solution along the length of the test section became very large, it was impossible to have the electrochemical reaction proceeding under mass transfer controlling conditions at all points on the surface of the test section. The increased conductivity of the electrolyte, the low concentration of iodine, and the upstream anode were all used to lower the voltage drop between the upstream and downstream edges of the test section.

The time averaged value of the mass transfer coefficient, $\overline{K}$, was calculated by averaging the local K from 22 electrodes at two different Reynolds numbers. The local mass transfer coefficient was calculated from Eq. 1 where I is the measured quantity and A, C_B, and n_e are known properties

of the system and solution. The fluctuations, $k = K - \overline{K}$, were determined by electrically subtracting out the signal representing $\overline{K}$.

The correlation coefficient of k or γ in the transverse direction, z, is defined as

$$R_{kk}(\Delta z) = \lim_{T\to\infty} \frac{1}{T} \int_{-T/2}^{T/2} k(t,z)k(t,z + \Delta z)\, dt. \quad (2)$$

It can be approximated by

$$R_{kk}(i\Delta z) = \frac{1}{j-1} \sum_{j=1}^{J-i} \frac{1}{N} \sum_{n=1}^{N} k(n,j)k(n,j+1), \quad (3)$$

where N is the number of samples in time, J is the number of probes separated by Δz in the transverse direction, and $k(n,j)$ and $k(n,j+1)$ are discreet measurements of the mass transfer coefficient at a particular time and location.

The spectra of k or γ are defined as the Fourier transform of the temporal correlation, $R_{kk}(\tau)$ or $R_{\gamma\gamma}(\tau)$,

$$W_k(\omega) = \int_{-\infty}^{+\infty} 2 \cdot R_{kk}(\tau) e^{-i\omega\tau}\, d\tau, \quad (4)$$

where ω is the frequency in radians per unit time. It follows from Eq. 4 that

$$2 \cdot \overline{k^2} = \frac{1}{2\pi} \int_{-\infty}^{+\infty} W_k(\omega)\, d\omega. \quad (5)$$

The spectral function, $W_k(\omega)$, was calculated by using fast-Fourier transform techniques (Welch, 1967).

Conditional sampling of the mass transfer data was carried out to determine the spatial scale of mass transfer fluctuations of large energy. The methods used were similar to those discussed by Hogenes (1979).

Certain samples were selected to use in computing an average spatial structure and its average duration. The samples had to meet two criteria to be used in this particular conditional average. First, the spatial location where the local fluctuating mass transfer coefficient goes from positive to negative is to occur between probes 5 and 6. Therefore $k(n,5)$-$k(n,6)$ is a negative number, where $k(n,j)$ represents the measurement of the mass transfer coefficient at the j^{th} probe during the n^{th} sample. Secondly, the energy of the fluctuations is to be relatively large,

$$2 \cdot (k(n,4) - k(n,7)) + (k(n,5) - k(n,6)) > m$$

where m was selected so that about 10% of the samples were included in the conditional average. The selected sample and the 12 samples preceding and following it in time are defined as an event. About 50 events were included in the conditional average.

RESULTS

Measurements of $\overline{K}$, $\overline{k^2}$, and of $W_k(\omega)$ made in the 20-cm pipe are compared with results obtained by Shaw and Hanratty (1977a) in a 2.54-cm pipe in Figures 5, 6 and 7. For comparison the spectral density function of $W_\gamma(\omega)$ is also plotted in Figure 7. As noted in earlier papers the fluctuating mass transfer rate at the wall is of much lower frequency than the fluctuating velocity field. This is illustrated in Figure 8 where typical $k(t)$ and $\gamma(t)$ signals are plotted.

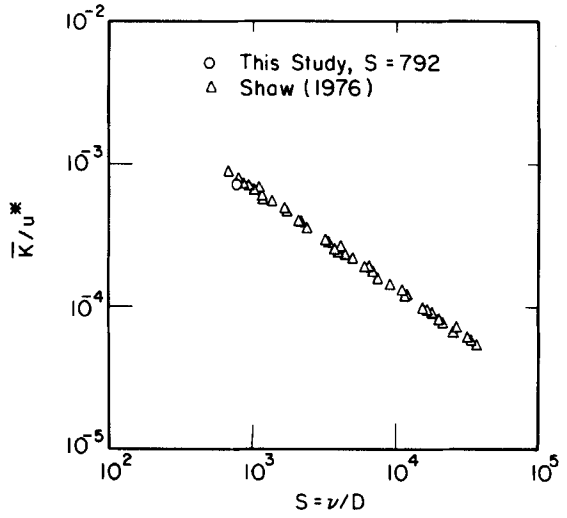

Figure 5. Comparison of measurements of the average mass transfer coefficient for a 20-cm pipe and a 2.54-cm pipe.

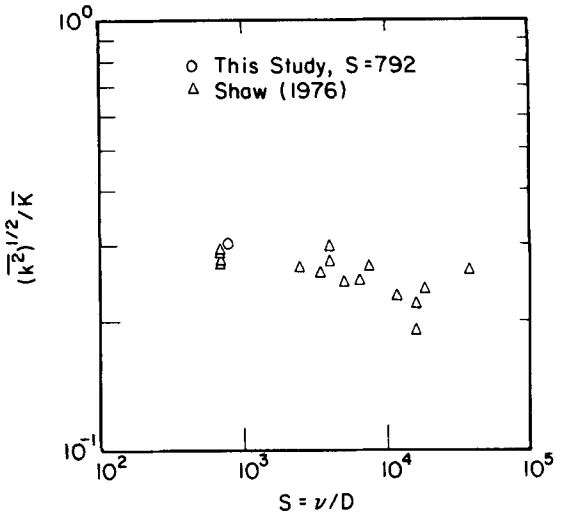

Figure 6. Comparison of measurements of the relative intensity of the fluctuations of the mass transfer coefficient for a 20-cm pipe and a 2.54-cm pipe.

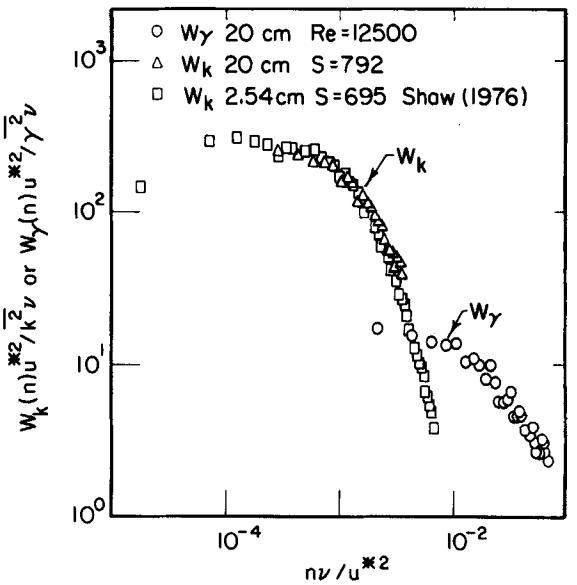

Figure 7. Comparison of mass transfer spectra in a 20-cm pipe and a 2.54-cm pipe with the spectrum of the transverse component of the velocity gradient.

The median frequency of the mass transfer fluctuations at a Schmidt number of 1,000 is found to be $\omega\nu/u^{*2} = 0.0075$. At a Reynolds number of 20,000, this corresponds to a frequency $n = \omega/2\pi$ equal to $\cong$ 2.4 Hz for the 2.54-cm pipe and $\cong$ 0.039 Hz for the 20-cm pipe. The total residence time of the fluid in the 20-cm pipe is 170 s at this Reynolds number. The extremely low values of the frequencies characterizing mass transfer to a wall at large Schmidt numbers raises the question whether these measurements are being strongly influenced by detailis of the design of the systems. The good agreement between the results for the 20-cm and 2.54-cm pipes suggest that this is not the case and that the fluctuations in K are related to universal turbulence properties.

Measurements of the spatial correlation of k are shown in Figure 9. For small z good agreement is obtained between measurements in the 20-cm and 2.54-cm pipes. However, at large z the results obtained by Shaw and Hanratty (1977a) are thought to be more

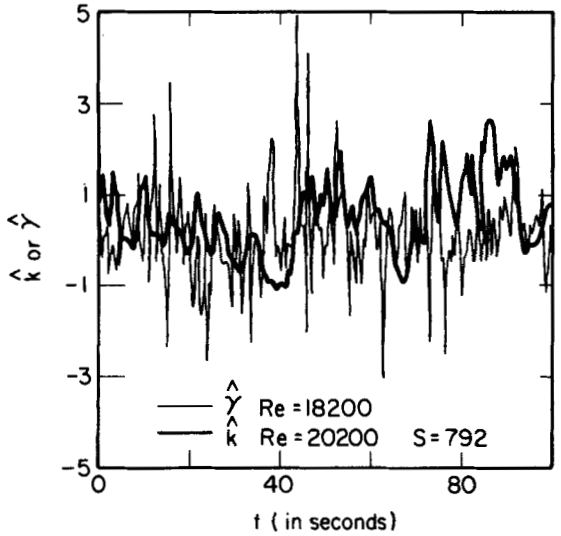

Figure 8. Comparison of velocity and mass transfer fluctuations in the 20-cm diameter flow loop.

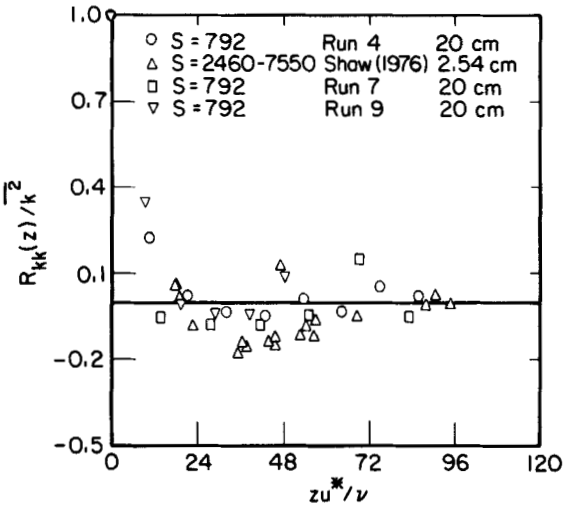

Figure 9. Measured correlations of the mass transfer coefficient in the transverse direction.

reliable because of the larger number of samples over which the average was taken.

The most important aspect of these measurements to be noted is that R_{kk} crosses zero at $zu^*/\nu \cong 20$. This is to be compared with the zero crossing at $zu^*/\nu \cong 33$ obtained for the correlation of the velocity measurements, $R_{\alpha\alpha}$ or $R_{\gamma\gamma}$, obtained by Hogenes (1979). It suggests that the mass transfer fluctuations are characterized by a small transverse scale, as has been found for the velocity field. In order to depict a typical wave pattern for the mass transfer field, as has been done by Hogenes (1979) for the velocity field, the multipoint mass transfer measurements were conditionally sampled for a large positive slope going through zero and for a large negative slope using the techniques described in the previous section. The time at which the condition for sampling was satisfied is designated as $t = 0$. Sixty-three events for a negative slope and 43 events for a positive slope were selected. The duration of an event was about $t^+ = 250$. Therefore, the duration of all events detected constituted about 10% of the total number of samples. The averages of the measurements from these two sets of events over a period extending from $tu^{*2}/\nu = -125$ to $tu^{*2}/\nu = +125$ are shown in Figure 10. A characteristic transverse wavelength can be estimated as twice the distance between a minimum and a maximum. In this way we get $\lambda_k^+ = 60$. This is to be compared with the value of $\lambda^+ \cong 100$ found in various ways for the velocity field.

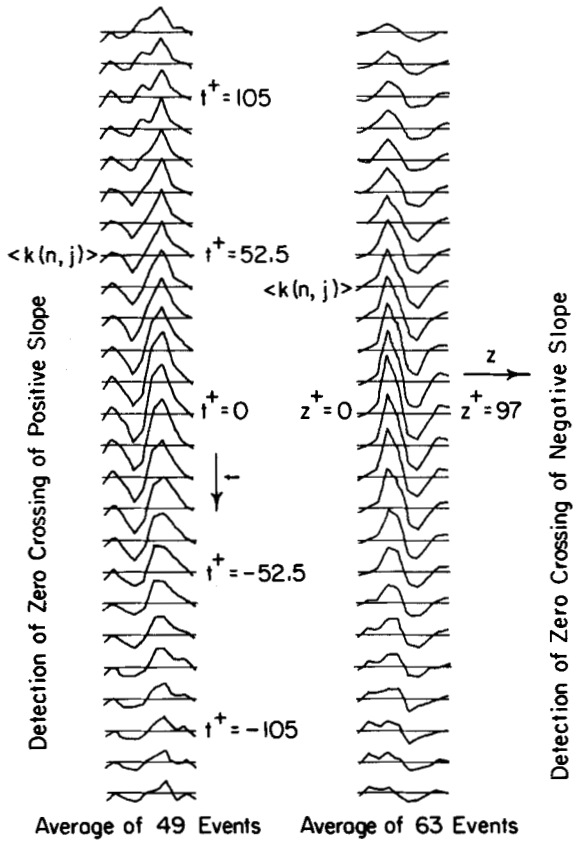

Figure 10. Conditional sampling of the mass transfer coefficients measured from an array of probes at a fixed axial location on the pipe wall.

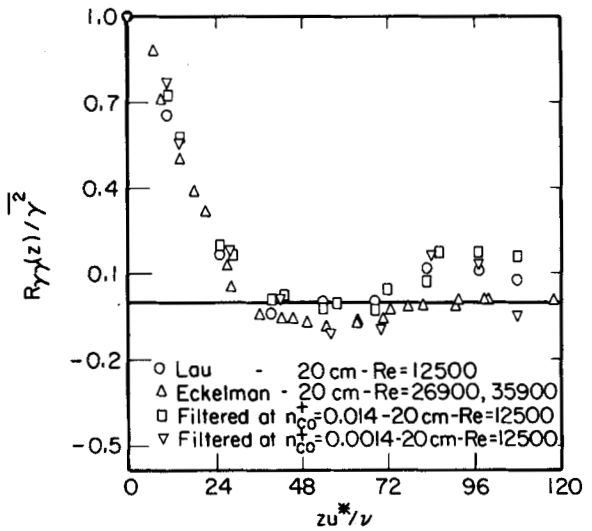

Figure 11. Correlation coefficient of the transverse component of the velocity gradient at the wall with varying amounts of the high frequency portion removed.

As pointed out in the introduction, the measurements of the spatial correlation of the fluctuating velocity field are dominated by frequencies much larger than those characterizing the mass transfer fluctuations. Figure 7 indicates it would be of interest to examine the scale associated with frequencies of $n\omega/u^{*2} \cong 0.0014$.

Figure 11 compares spatial correlations of measurements of the velocity gradient that have been filtered at $n\omega/u^{*2} = 0.014$ and at $n\omega/u^{*2} = 0.0014$ with those obtained from unfiltered signals. Figure 12 shows the effect of this low pass filtering on the time variation of γ at a given location. Figure 13 shows the effect of this filtering on the simultaneous measurements of γ at a number of

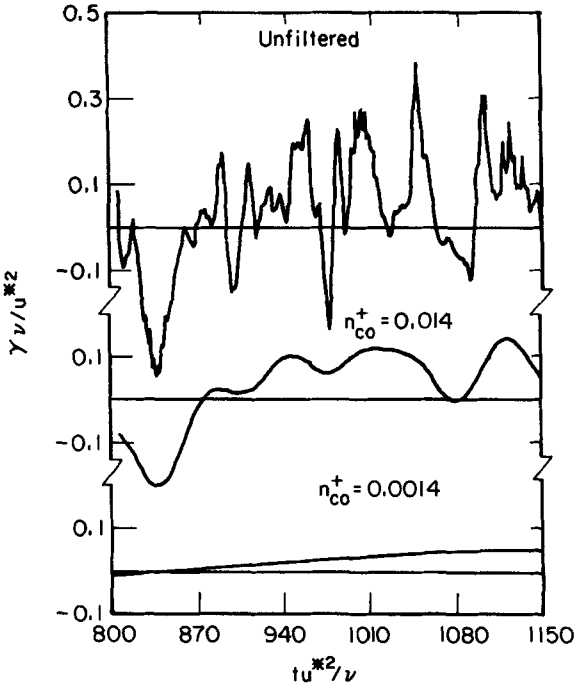

Figure 12. Effect of filtering on the time variation of the transverse component of the wall velocity gradient in a 20-cm pipe, *Re* = 12,500.

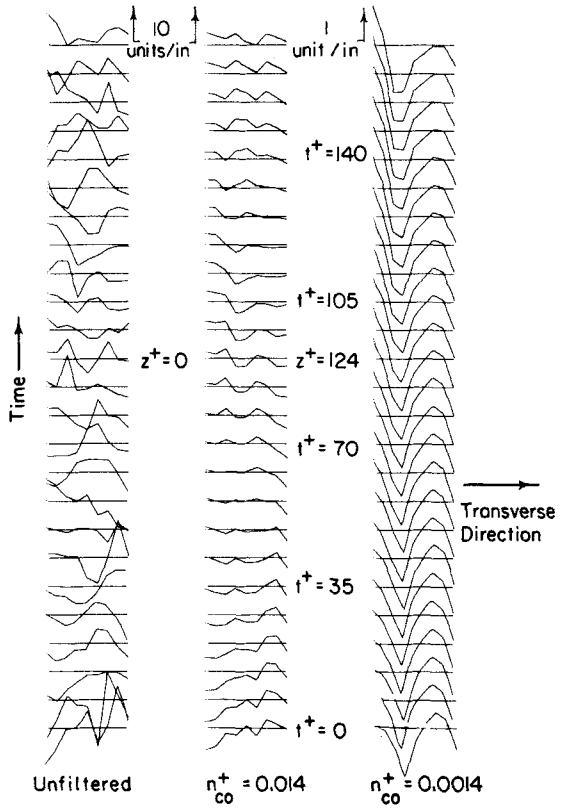

Figure 13. Effect of filtering on the spatial variation of the transverse component of the wall velocity gradient, γ.

z locations. The first column in Figure 13 shows the considerable change that is observed in the γ-pattern over a time interval $tu^{*2}/\nu = 175$. However it is noted that the pattern displayed by signals that have been low pass filtered at $n\nu/u^{*2} = 0.0014$ shows little temporal change but a spatial wavelength of $\lambda^+ = 90$. This means that no matter which portion of the velocity (high or low frequencies) controls the mass transfer the spatial scale will remain the same.

An examination of results such as shown in Figure 13 and of the measured correlation coefficients shown in Figure 11 clearly show that the transverse spatial scale of the low frequency velocity fluctuations is of the same magnitude as the spatial scale of the most energetic velocity fluctuations. Since large mass transfer rates are experienced at locations of intense inflows or outflows, the wavelength λ_k^+ should be approximately $\frac{1}{2}$ of the wavelength of the eddies controlling mass transfer; that is, the measurements of the lateral extent of the mass transfer fluctuations and the velocity gradient fluctuations should be close in magnitude, but not exactly equal. Our measurements suggest $\lambda^+ \cong 60$ for the mass transfer fluctuations and $\lambda^+ \cong 90$–100 for velocity gradient fluctuations of a range of frequencies.

We conclude that measurements do not contradict the notion that turbulent mass transfer to a solid boundary at large Schmidt numbers is controlled by velocity fluctuations of much lower frequency than those containing most of the energy.

ACKNOWLEDGMENT

This work is being supported by the National Science Foundation under Grant NSF CPE 79-20980.

NOTATION

A = surface area of cathode, cm^2
C_B = bulk concentration of specie, mol/cm^3
F = Faraday's constant - 96,500, coul/eq
I = current, coul/s
k,K = fluctuating and total mass transfer coefficient, cm/s
n = frequency in Hz, L/s
n_{co} = cut off frequency used in low pass filtering in Hz, L/s
n_e = equivalents per mole of reactant in electrolytic reaction, eq/mol
$R_{kk}(\tau)$ = auto-correlation of k, cm^2/s^2
$R_{kk}(\Delta z)$ = spatial correlation of k in the transverse direction, cm^2/s^2
S = Schmidt number = ν/D
t = time, s
T = time or period of dominant velocity fluctuations, s
u^* = friction velocity, cm/s
u,v,w = components of the velocity
$W_k(\omega)$ = spectrum of k, cm^2/s
$W_\gamma(\omega)$ = spectrum of γ, L/s
y = coordinate normal to the wall, cm
z = coordinate in the transverse direction, cm

Greek Letters

α = velocity gradient in the streamwise direction evaluated at the wall, L/s
β = ν/y^2
γ = velocity gradient in the transverse direction at the wall, L/s
δ_c = thickness of the concentration boundary-layer, cm
λ = wavelength in transverse direction of dominant flow structure, cm
λ_k = wavelength in transverse direction of dominant structure of mass transfer, cm
ν = kinematic viscosity, cm^2/s
τ = time delay used in auto-correlation, s
ω = circular frequency, L/s

Symbols

$-$ = time average quantity
$+$ = quantity made dimensionless with u^* and ν

LITERATURE CITED

Campbell, J. A., "The Velocity-Concentration Relationship in Mass Transfer to a Wall," Ph.D. Thesis, University of Illinois, Urbana (1981).

Campbell, J. A., and T. J. Hanratty, "Mass Transfer Between a Turbulent Fluid and a Solid Boundary: Linear Theory," *AIChE J.*, p. 988 (Nov., 1982).

Fortuna, G., and T. J. Hanratty, "The Influence of Drag-reducing Polymers on Turbulence in the Viscous Sublayer," *J. Fluid Mech.*, **53**, 575 (1972).

Hogenes, J. H. A., "Identification of the Dominant Flow Structure in the Viscous Wall Region of a Turbulent Flow," Ph.D. Thesis, University of Illinois, Urbana (1979).

Lee, M. K., L. D. Eckelman, and T. J. Hanratty, "Identification of Turbulent Wall Eddies Through the Phase Relation of the Components of the Fluctuating Velocity Gradient," *J. Fluid Mech.*, **66**, 17 (1974).

Mitchell, J. E., and T. J. Hanratty, "A Study of Turbulence at a Wall Using an Electrochemical Wall-Stress Meter," *J. Fluid Mech.*, **26**, 199 (1966).

Reiss, L. P., "Investigation of Turbulence Near a Pipe Wall Using a Diffusion Controlled Electrolytic Reaction on a Circular Electrode," Ph.D. Thesis, University of Illinois, Urbana (1967).

Reiss, L. P., and T. J. Hanratty, "Measurement of Instantaneous Rates of Mass Transfer to a Small Sink on a Wall," *AIChE J.*, **8**, 245 (1962).

Reiss, L. P., and T. J. Hanratty, "An Experimental Study of the Unsteady Nature of the Viscous Sublayer," *AIChE J.*, **9**, 154 (1963).

Sirkar, K. K., "Turbulence in the Immediate Vicinity of a Wall and Fully Developed Mass Transfer at High Schmidt Numbers," Ph.D. Thesis, University of Illinois, Urbana (1969).

Sirkar, K. K. and T. J. Hanratty, "The Limiting Behavior of the Turbulent Transverse Velocity Component Close to a Wall," *J. Fluid Mech.*, **44**, 605 (1970).

Shaw, D. A., and T. J. Hanratty, "Influence of Schmidt Number on the Fluctuations of Turbulent Mass Transfer to a Wall," *AIChE J.*, **23**, 160 (1977a).

Shaw, D. A., and T. J. Hanratty, "Turbulent Mass Transfer Rates to a Wall for Large Schmidt Numbers," *AIChE J.*, **23**, 28 (1977b).

Van Shaw, P., and T. J. Hanratty, "Fluctuations in the Local Rate of Turbulent Mass Transfer to a Pipe Wall," *AIChE J.*, **10**, 475 (1964).

Welch, P. D., "The Use of Fast Fourier Transform for the Estimation of Power Spectra: A Method Based on Time Averaging Over Short, Modified Periodograms," *IEEE Trans. on Audio and Electroacoustics*, **15**, 70 (1967).

Manuscript received July 10, 1981; revision received April 2, and accepted April 19, 1982.

Mechanism of Turbulent Mass Transfer at a Solid Boundary

Mass transfer between a turbulent fluid and a solid boundary is considered for the case of large Schmidt numbers. The variation of the mass transfer coefficient with time, $K(t)$, is calculated by solving the mass balance equation using a random velocity input. An interpretation of the mass transfer process which is radically different from that given by classical approaches is obtained.

J. A. CAMPBELL and T. J. HANRATTY

University of Illinois
Urbana, IL 61801

SCOPE

The goal of a theory of turbulent mass transfer is to relate the mass transfer rate at a solid boundary to measurable properties of the fluctuating velocity field. For large Schmidt numbers, this is simplified because the concentration boundary layer is so thin that only the limiting behavior of the velocity field close to the solid surface needs to be considered. Solutions of a linearized form of the mass balance equations (Campbell and Hanratty, 1981a) have suggested a theory which is quite different from classical approaches. It shows that the mass transfer boundary layer acts as a filter in that only low frequency velocity fluctuations containing a small fraction of the turbulent energy are controlling the mass transfer process. However, this interpretation is open to question, since a number of the results obtained from the linear theory analysis are not satisfactory. The calculated dependency of the mass transfer coefficient on Schmidt number, $\overline{K} \sim S^{-3/4}$, does not agree with experiment and calculated intensities of the mass transfer fluctuations are much too high. In the research described in this paper, numerical solutions of nonlinear forms of the mass balance equations were carried out using a random input for the velocity field. The results of this calculation appear as a randomly varying mass transfer coefficient, $K(t)$, and a randomly varying concentration field, $C(y,t)$. The statistical properties of these results can then be compared with experiment.

Two types of nonlinear model equations were explored. In one of these, only normal velocity fluctuations, $v(y,t) = \beta(t)y^2$, are considered. In the other, the influence of the transverse velocity fluctuations is included by using a velocity field which is periodic in the transverse direction.

CONCLUSIONS AND SIGNIFICANCE

The results of these calculations confirm the picture of turbulent mass transfer at a solid boundary presented by the solutions of the linear mass balance equations. Only velocity fluctuations of low frequency are influencing the mass transfer rate. There is no observable difference betwee mass transfer rates calculated from a velocity input containing a spectrum of frequencies and those calculated from a velocity input containing only low frequencies (Figure 5).

There are, however, interesting differences between the linear and nonlinear calculations. For the linear case, the frequency